FEATURE ARTICLE

Modeling Electrochemical Interfaces in Ultrahigh Vacuum: Molecular Roles of Solvation in Double-Layer Phenomena

Ignacio Villegas[†] and Michael J. Weaver*

Department of Chemistry, Purdue University, West Lafayette, Indiana 47907

Received: July 25, 1997; In Final Form: September 30, 1997[⊗]

Some virtues of modeling electrochemical systems by dosing interfacial components onto clean metal surfaces in ultrahigh vacuum (UHV) are discussed, with an emphasis on elucidating the nature of double-layer solvation and how solvent molecules influence the intermolecular interactions. This "*non situ*" strategy (as distinct from ex situ approaches involving electrode transfer to/and from UHV) allows each interfacial component (solutes, ions, solvent) to be added sequentially and in controlled amounts, enabling the various molecular (and hence intermolecular) ingredients that constitute the double layer to be accessed in *incremental* fashion. The approach also provides an invaluable means of understanding the differences in structure and bonding between analogous electrochemical interfaces and the constituent metal−UHV systems. Such issues are particularly germane with the recent advent of microscopic-level structural information for in situ electrochemical systems. Described specifically here is the UHV-based vibrational characterization of solvent and chemisorbate modes by employing infrared reflection−absorption spectroscopy (IRAS), together with work-function measurements, as a function of interfacial composition. The former provides a sensitive monitor of intermolecular interactions as well as being applicable (albeit with more restrictions) to in situ systems, whereas the latter yields insight into surface-potential profiles and also links the potential scales of metal−UHV and electrochemical interfaces. Several distinct examples aimed at elucidating double-layer solvation effects on Pt(111), recently scrutinized in our laboratory, are discussed. These include examining the progressive solvation of cations, adsorbed anions, and combinations thereof, by water and methanol. Comparisons with vibrational spectra for the solvation of gas-phase (i.e., isolated) ions enables the substantial influence of the metal surface upon double-layer solvation to be explored in detail. The converse role of double-layer charge upon the inner-layer solvent orientation (as exemplified for acetone and acetonitrile) is also found to be considerable and involves long-range forces. The combined influences of solvent and double-layer charge upon chemisorbate structure and bonding are also considered for the archetypical example of carbon monoxide. Marked electrostatic effects of solvation upon CO structure and bonding are seen even in the absence of net charge. The complex short-range influences of added cationic (K^+) charge upon the CO adlayer are quenched upon partial K^+ solvation. The longer-range electrostatic effects are progressively modified as the chemisorbate layer as well as the ionic charges become fully solvated, so to reveal a simple "Stark-tuning" frequency−potential behavior identical with that familiar in electrochemistry. Some more general implications and applications of such "UHV double-layer modeling" tactics are also briefly considered.

1. Introduction

Understanding the nature of intermolecular interactions at metal−electrolyte interfaces forms a centrally important theme in electrochemistry. The significance of this issue is self-evident upon the recognition that such electrochemical interfaces include generally three types of components—solvent, ions, and adsorbed (or chemisorbed) solute—in addition to the metal and attendant electronic charge. Consequently, gaining an appreciation of the manner in which these entities naturally interact, especially regarding the molecular role of the solvent in both modifying and mediating the structure and energetics of charge−solute and related interactions, constitutes an issue having exemplary fundamental and practical significance.

The past decade or so has witnessed remarkable progress in our ability to characterize experimentally the structure of electrochemical interfaces on the atomic/molecular level.[1,2] Such developments have been driven in particular by the emergence of an increasing swath of in situ microscopic and spectroscopic techniques, that is, having the ability to examine complete electrochemical interfaces under electrode-potential control and even during the occurrence of electron transfer or other surface processes.[1,2] Prominent among these methods are scanning tunneling microscopy (STM) and surface X-ray scattering (SXRS), capable of scrutinizing the spatial arrangement of atoms and molecules at ordered electrochemical interfaces, and a trio of techniques that yield vibrational information for adsorbates. The latter group, comprising infrared reflection−absorption spectroscopy (IRAS), surface-enhanced Raman scattering (SERS), and visible-infrared sum frequency generation (SFG), have markedly different strengths and weaknesses. While SERS offers unique surface sensitivity and freedom from bulk-phase interferences, which are especially significant attributes for electrochemical systems, both IRAS and SFG, but not SERS,

[†] Present address: Department of Chemistry, University of New Mexico, Albuquerque, NM 87131.

[⊗] Abstract published in *Advance ACS Abstracts,* November 1, 1997.

S1089-5647(97)02441-3 CCC: $14.00

are applicable to ordered single-crystal as well as polycrystalline surfaces. This latter capability renders IRAS, and very recently SFG, as sought-after methods for characterizing adsorbates at atomically uniform metal−gas and metal−ultrahigh-vacuum (UHV) interfaces. Indeed, the applicability (and application) of methods such as STM and IRAS to analogous ordered metal surfaces in both in situ electrochemical and UHV environments is promoting firm ties between these formerly disconnected segments of surface science.[1−3]

The upsurge of interest in metal−UHV surface science in the late 1960s/1970s, spurred by the emergence of a variety of powerful surface characterization methods, also encouraged the development of UHV-based experimental strategies aimed at electrochemical systems. The first variant involves the transfer of electrode surfaces between the electrochemical cell and a UHV chamber. This so-called "ex situ" approach, pioneered especially by Hubbard and co-workers,[3] has the considerable virtue of enabling (in principle) the full range of UHV-based characterization techniques to be harnessed for the structural examination of actual electrode surfaces. On the other hand, the ambient-temperature surface transfer necessitated by experimental constraints results in the evaporation of some double-layer components, especially solvents, in the UHV environment, so that such ex situ strategies are generally limited to scrutinizing chemisorbed and other nonvolatile interfacial species.

A quite distinct UHV-based approach for exploring electrochemical systems entails building electrochemically relevant interfaces in vacuum by sequential gas-phase dosing onto an initially clean surface of all the various components that together constitute the double layer. This so-called "non situ" strategy,[4] pioneered by Sass and co-workers during the 1980s,[5] is often known as "UHV electrochemical (or double-layer) modeling".[6] Most significantly, the approach can yield unique insight into the nature of interfacial intermolecular interactions. Exploring the spectral and other structure-sensitive responses to judiciously chosen variations in the interfacial composition can provide detailed information regarding the specific roles of each double-layer ingredient, thereby furnishing an integrated stepwise link between the inherently multicomponent electrochemical interfaces and constituent metal−UHV systems. While low temperatures (below ca. 150 K) are typically required to prevent evaporation of volatile components, especially solvents, the fundamental nature of ion−solvent and other double-layer interactions should be insensitive to temperature. Furthermore, examining the temperature-induced desorption (i.e., undertaking temperature-programmed desorption, TPD) of individual components can lend insight into the energetics of interfacial interactions.

Consequently, while the recent emergence of in situ microscopic methods now enables the spatial structure and bonding at actual electrochemical interfaces to be probed directly, there are still persuasive reasons to pursue such UHV-based studies. Indeed, the availability of an increasingly rich swath of in situ structural information *encourages* related measurements at metal−UHV interfaces as a means of deciphering the more complex molecular-level behavior of electrochemical interfaces uncovered by the former approaches. Moreover, there remain some key facets of double-layer phenomena, such as solvation, that are difficult or even impractical to examine with currently available in situ methods, yet can be explored in detail at model electrochemical interfaces in UHV.

Reflecting the above developments, a topic of central recent interest in our laboratory involves the structural and dynamical characterization of ordered metal−solution interfaces by utilizing in situ microscopic-level techniques, especially IRAS and STM, in conjunction with conventional electrochemical methods.[1] The acquisition of such in situ information highlighted to us some intriguing differences as well as similarities between the structural properties of ostensibly related electrochemical and metal−UHV interfaces. For example, the coverage-dependent vibrational properties of carbon monoxide adsorbed at ordered Pt-group electrodes can be markedly different in comparison with chemisorption on the clean metals in UHV.[1c,7,8] The dissimilarities include differences in adsorbate binding geometries as well as more subtle distinctions in vibrational frequencies and implicate the importance of the other double-layer components (solvent, ions, electronic charge) in modifying or even controlling the chemisorbate structure and bonding.[6,7]

These and other observations encouraged us to initiate UHV double-layer modeling experiments, with a prominent initial objective being the elucidation of the coupled influences of solvation and electrostatic factors upon the molecular structure of such ordered metal−solution interfaces. We have focused on UHV-based infrared spectral characterization along with work-function measurements. In addition to providing detailed information regarding intermolecular interactions via the intramolecular vibrational properties of solvent and chemisorbate species, the former also provides a direct connection to in situ electrochemical interfaces since IRAS is applicable also in the latter environment (albeit with more restrictions arising from bulk-phase solvent interferences). The latter measurements yield valuable insight into the surface-potential profile as a function of the interfacial composition, as well as furnishing a link to the surface potentials developed at the corresponding in situ electrochemical interfaces.[4−6]

The aim of the present Feature Article is to outline some applications of UHV double-layer modeling tactics for exploring intermolecular interactions in electrochemical systems, illustrated primarily by recent experimental results obtained in our laboratory. Emphasis is placed on understanding the molecular essence of interfacial solvation as deduced primarily from vibrational spectral data and how the solvent modifies, and is modified by, adsorbed solute and double-layer charges.

2. Relationship between UHV Model and Electrochemical Surface-Potential Scales

As enunciated originally by Sass et al.,[5] evaluations of the changes in surface potential, $\Delta\phi^M$, engendered by alterations in the surface composition of UHV model interfaces are anticipated to yield valuable insight into the molecular-level origins of the electrostatic fields generated at electrochemical interfaces. It is therefore appropriate to clarify first the relationship between such surface-potential scales in UHV and in situ electrochemical environments. A particularly enlightening (and detailed) discussion of this issue is contained in ref 6a.

As is well documented,[6a,9] it is strictly not possible to evaluate the surface potential drop, ϕ^M, across a single metal−vacuum or metal−solution interface. Nevertheless, the metal work function, Φ^M, that is, the work required to remove an electron from the bulk metal to a point just outside in vacuum,[6a] is certainly measurable for the former interfaces. While Φ^M contains a "bulk metal" contribution as well as the "surface component", $e\phi^M$, the former is a constant for a given metal phase, so that measured adsorbate-induced changes in Φ^M, $\Delta\Phi^M$, can be identified directly with alterations in the surface potential drop, $e\phi^M$. For in situ electrochemical interfaces one usually employs a reference electrode rather than the work-function "vacuum reference", yielding the well-known electrode potential scale, E^M. What, then, is the relationship between Φ^M

and E^M values for a given pair of metal−vacuum and metal−solution interfaces or, more pointedly, for a "model electrochemical" interface in UHV?

Given that the E^M values are necessarily referred to a reference electrode (by convention the aqueous normal hydrogen electrode, NHE), the corresponding Φ^M value for the single electrochemical interface can be found if the "work function" of the reference electrode (Φ_{ref}) is known. The latter is commonly described in terms of the so-called "absolute" potential of the reference electrode, E_k, where $\Phi_{ref} = eE_k$.[9] Consequently, one can relate the E^M and Φ^M values for a given interface by[9]

$$E^M = \Phi^M/e - E_k \quad (1)$$

Equation 1 therefore provides the desired conversion of the reference state for electrochemical interfaces from the NHE (or other reference electrode) to the "vacuum level" obliged for metal−UHV interfaces.

The Φ^M value for an actual electrochemical interface will equal the measured work function for the corresponding metal−vacuum interface when the latter is modified by the presence of a liquid layer possessing the same electrostatic properties as in the former system.[10] (These "electrostatic properties" include the potential drops across the metal−solution and solution−vacuum interfaces, $\phi^M{}_S$ and χ_S, respectively.) Consequently, then, measurements of Φ^M for a given "UHV electrochemical model" interface, containing work-function shifts $\Delta\Phi^M$ induced by the addition of components (solvent, ions, etc.) of the electrochemical double layer, can be linked directly to electrode potential values for the corresponding "real" metal−solution interface, E^M, provided that E_k is known. The comparison is undertaken most simply for interfaces having zero electronic charge, σ_m, such as UHV systems containing only dipolar chemisorbate and solvent, whereupon both Φ^M and E^M will refer to the "potential of zero charge". Higher or lower values of Φ^M and E^M will then correspond to positive or negative σ_m values, respectively.

A conceptually unexpected difficulty, however, is that two significantly disparate groups of E_k estimates have been deduced for the NHE, one about 4.45 V and the other around 4.8 V.[6a,11] The former estimate was deduced partly on thermodynamic grounds,[9] whereas the latter values were extracted chiefly from electrode emersion experiments into UHV.[11] While arguments have been forwarded for and against either the lower or higher E_k estimates, the actual situation remains unclear.[6a] Given that the reliability of the latter E_k estimate suffers from solvent evaporation upon electrode transfer into UHV, the ca. 0.4 V higher value could be connected with the removal of the solvent dipole contribution to $\phi^M{}_S$. Evidence favoring this explanation is gleaned from the known ϕ^M decreases, ca. 0.7−1 V, attending water adsorption in UHV together with the observation that Au or Pt electrodes emersed into damp nitrogen (and therefore retaining an aqueous film) yield Φ^M values that are ca. 0.3 V *lower* than for the in situ electrodes.[6a,12] On the other hand, this picture is clouded by the observation of E_k estimates around 4.8 V in some experiments where the surface presumably maintains a water film even after ambient-temperature emersion.[6a]

One estimate of E_k worth mentioning in the present context was derived by matching potential-dependent vibrational frequencies, ν_a, for a given probe adsorbate at corresponding UHV model and in situ electrochemical interfaces.[13] This procedure exploits the well-known sensitivity of such vibrational frequencies to the surface potential (the so-called "Stark tuning" effect[7b,14,15]), so that the E^M value that yields a ν_a value equal to that at the UHV model interface should correspond to Φ^M for the latter. The specific system in ref 13, a saturated NO adlayer on Pt(111) in aqueous solution, was chosen in view of the adsorbate stability toward electrooxidation at the high potentials necessary for comparison with the uncharged Pt(111)−water UHV interface. This comparison yielded a E^M value of 0.5 V vs NHE, corresponding to $\Phi^M = 5.4$ eV for the hydrated UHV interface; from eq 1, one obtains $E_k \approx 4.9$ V. The analysis is only approximate and may be complicated by differences in the interfacial water structure, and hence in $\phi^M{}_S$ and χ_S, between the ambient-temperature electrochemical and low-temperature (90 K) UHV environments. This finding nonetheless suggests that E_k values around 4.8 V may be appropriate when applying eq 1 in the context of UHV electrochemical modeling studies. Comparable E_k values, ca. 4.6 V, have been deduced from related Stark-tuning analyses with carbon monoxide adlayers[16,17] (vide infra).

We now consider some illustrative examples, taken chiefly from our recent work, of applying UHV double-layer modeling tactics by using combined IRAS/work-function measurements on Pt(111) to elucidate interfacial solvation effects in electrochemistry. The Pt(111) surface was chosen in view of its previous detailed characterization in both UHV and electrochemical environments, along with a strong propensity for chemisorption and catalytic chemistry. Discussion will be limited to an overview of key findings; experimental details can be found in the references cited.

3. Interfacial Ion−Solvent Interactions

A typical, as well as relatively simple, situation in interfacial electrochemistry involves the double layer containing chiefly only a single type of ionic countercharge along with the solvent. Such a circumstance is commonly encountered at potentials below the potential of zero charge (E_{pzc}) where the excess electronic charge at the metal surface (σ_m) is balanced primarily by cation countercharges (σ_+). Following Sass[5] and others,[17] we have chosen to model this case in UHV by employing alkali metal cations, specifically K^+. This choice arises in part from the formation of interfacial K^+ upon K atom dosing, together with the availability of an accurate coverage assay from the large linear Φ^M decreases induced on Pt(111) in the coverage regime, $\theta_K \leq 0.08$, of electrochemical interest.[18] Light alkali metal cations also provide archetypical cases of nonspecifically adsorbed ions in electrochemistry.

3.1. Progressive Cation Solvation: Comparison with Gas-Phase Systems. One of the attributes of UHV double-layer modeling is the ability to delineate the various stages of ion solvation (or other interactions) by progressive controlled dosing of solvent molecules onto the surface. We now consider the work-function and IRAS responses to the progressive K^+ solvation on Pt(111) by two hydrogen-bonded molecules, water and methanol, and two aprotic dipolar solvents, acetonitrile and acetone. Adsorption of the former pair is dominated by hydrogen-bonded intermolecular interactions, while more clear-cut metal surface−solvent interactions are evident spectroscopically for the latter. One intriguing aspect, considered below, is the opportunity to compare such infrared spectra for progressive *interfacial* cation solvation with vibrational data for the corresponding sequential solvation of gas-phase (i.e., isolated) cations. Differences in these spectral responses as a function of the solvent−ion stoichiometry can shed light on the manner in which the metal surface modifies the solvation of double-layer ions.[16,20]

Typical $\Delta\Phi^M$ responses to solvent dosing onto both clean and K^+-modified Pt(111) [referenced to the former state] for water, methanol, acetonitrile, and acetone at 100 K are depicted

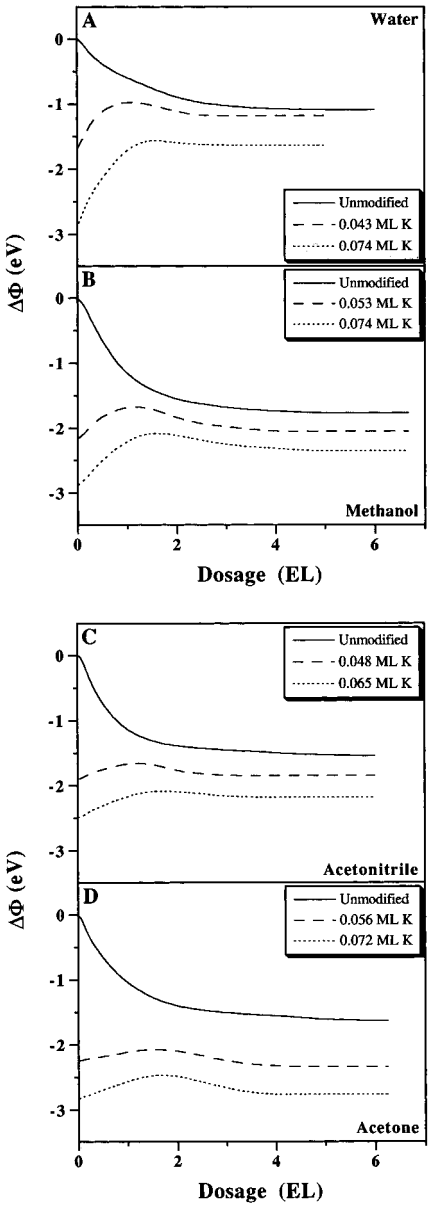

Figure 1. Changes in surface work function on Pt(111), $\Delta\Phi$, induced by increases dosages of (A) water, (B) methanol, (C) acetonitrile, and (D) acetone at 100 K in the presence of predosed coverages of potassium as indicated. Solvent dosages given in "equivalent layers" EL (see footnote 22). Data taken from refs 16 and 20.

in Figure 1A−D, respectively. (More detailed results are provided in refs 16 and 19−21; see also footnote 22.) The $\Delta\Phi$ measurements were made by using a Kelvin probe; they can be converted into absolute Φ^M (and hence also E^M) values by noting that the work function of clean Pt(111) is about 5.9 eV. In the absence of K^+, large (1−1.5 eV) Φ^M decreases are observed for increasing solvent dosages, θ_s*, that can be attributed to solvent-induced redistribution of charge in the metal surface as well as from net solvent dipole orientation (vide infra).[19] The presence of predosed K^+, however, triggers in each case nonmonotonic $\Delta\Phi^M-\theta_s$* responses, Φ^M *increasing* for solvent dosages below ca. 1.5 equivalent monolayers (Figure 1A−D).[22] This effect, observed previously for water dosing on alkali-modified surfaces,[5a,17,23] has been attributed to field-induced solvent dipole orientation next to the adsorbed cations. (Note that initial solvent dosing should yield preferentially cation rather than surface solvation on energetic grounds.)

More detailed insight into the nature of such cation−solvent interactions can be gleaned from infrared spectra obtained under

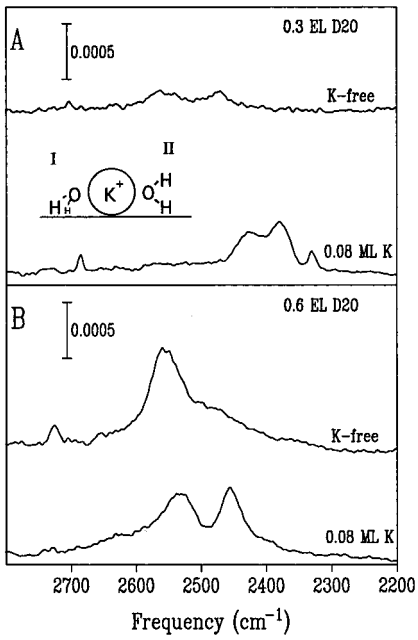

Figure 2. Infrared spectra in O−D stretch region for dosages of D_2O onto clean and K-modified Pt(111) at 100 K. Data taken from ref 16.

these progressive solvation conditions. Figure 2A,B shows examples of IRAS data obtained in the O−D stretch (ν_{OD}) frequency region for a pair of submonolayer dosages of D_2O onto both clean and K^+-modified ($\theta_K = 0.08$) Pt(111).[16] The K^+-free spectra show weak and broadened ν_{OD} bands that are red-shifted from the values for free D_2O ($\nu_s = 2671$ cm^{-1}, $\nu_{as} = 2788$ cm^{-1}), consistent with the formation of hydrogen-bonded water. The presence of K^+, however, yields striking changes in the spectra, especially at low water dosages. The water coverage, θ_W, in Figure 2A is 0.2 ML (one "equivalent monolayer" of water, the so-called "bilayer", corresponds to $\theta_W = {}^2/_3$), yielding a D_2O/K^+ stoichiometry (θ_W/θ_K) of 2.5, so that the water should be in the K^+ primary coordination shell. Multiple and extensively red-shifted ν_{OD} bands are seen, contrasting the situation for gas-phase metal ion hydration, which exhibits only smaller frequency shifts from uncoordinated water.[24]

This large (ca. 250−350 cm^{-1}) frequency downshift can be attributed to the water configurations sketched in Figure 2A, with at least one D atom hydrogen bonded to the metal surface along with cation−oxygen coordination, leading to O−D bond softening. Similar hydration configurations have been suggested for this system on the basis of surface vibrational data obtained by electron energy loss spectroscopy (EELS).[25] These data also show that the Pt−OH_2 vibration seen at 560 cm^{-1} on clean Pt is absent in the presence of K^+, confirming the dominant occurrence of cation hydration.[25]

The ν_{OD} band frequencies for K^+ interfacial hydration are upshifted markedly with increasing water dosages. The spectrum in Figure 2B, corresponding to a θ_W/θ_K ratio of 5, shows this effect clearly in comparison with Figure 2A. These changes can be attributed to a greater number of waters in the primary coordination shell, although the onset of a secondary solvation shell, hydrogen bonded to the first, is likely by this point. Eventually for large stoichiometric ratios, $\theta_W/\theta_K > 10$, metal surface as well as cation hydration predominates, as evidenced by the development of the typical broad ν_{OD} band around 2550 cm^{-1} associated with hydrogen-bonded networks.[16]

Figure 3A,B shows parallel representative IRAS data obtained for methanol solvation.[20] The observed behavior of the O−H stretching vibration (ν_{OH}) of methanol is closely similar to that

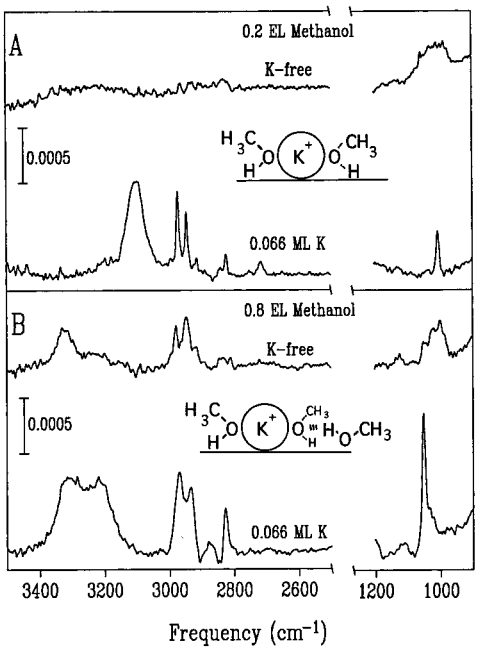

Figure 3. Infrared spectra in O−H and C−O stretch regions for methanol dosed on clean and K-modified Pt(111) at 100 K. Data taken from ref 20.

for water. Thus, the ν_{OH} band on the K^+-containing surface in Figure 3A, corresponding to a methanol/K^+ stoichiometry of ca. unity, is markedly red-shifted (by ca. 700 cm^{-1}) compared to gas-phase methanol, as well as being more intense than the (barely discernible) ν_{OH} feature seen for the same methanol dosage in the absence of K^+. As before, this finding is indicative of the occurrence of cation-solvation configurations as sketched in Figure 3A, involving −OH hydrogen bonding to the metal surface as well as oxygen coordination to the cation. The presence of K^+ also triggers the appearance of methyl C−H vibrations at 2945/2980 cm^{-1}, along with a sharpened C−OH stretching band, ν_{C-OH}, at 1007 cm^{-1} (Figure 3A). Increasing the methanol/K^+ ratio, as shown in Figure 3B for a stoichiometry of ca. 4.5, again results in substantial upshifts in the ν_{OH} frequency. The appearance of a pair of ν_{OH} bands under these conditions is tentatively ascribed to the emergence of secondary as well as primary cation solvation, as depicted in Figure 3B. Eventually, for methanol dosages above 1−1.5 EL, a single broad ν_{OH} feature at ca. 3280 cm^{-1} dominates, indicative of the formation of extensive interfacial solvation by a H-bound methanol network.

Further insight into the influence of the metal surface on the progressive cation−methanol solvation can be obtained by examining the behavior of the ν_{C-OH} band in comparison with corresponding vibrational data for the methanol solvation of gas-phase alkali cations reported by Lisy and co-workers.[20,26] In the former case, increasing the methanol/K^+ stoichiometry above 4, as in Figure 2B, results in the virtual replacement of the ca. 1010 cm^{-1} ν_{C-OH} band by a higher-frequency ν_{C-OH} feature at 1050 cm^{-1}, coinciding with the appearance of a higher-frequency ν_{OH} component. Given that such blue-shifted ν_{C-OH} bands are diagnostic of methanol acting as a proton donor,[27] this suggests the presence of cation/secondary solvation as depicted in Figure 3B, with the hydroxyl hydrogen H-bonded to the oxygen of the primary solvating methanol. The attenuation of the ca. 1010 cm^{-1} band under these conditions indicates that the primary solvation is also perturbed by this point.

Interestingly, this behavior is quite different to the vibrational behavior seen for the progressive methanol binding to gas-phase alkali cations, where the onset of secondary solvation yields lower-frequency ν_{C-OH} bands, consistent with the second methanol shell acting as a proton *acceptor*.[26] The opposite mode of H bonding in the interfacial case can readily be attributed to the influence of the metal surface if the hydroxyl hydrogen of the primary solvating methanol is H bound to the surface (Figure 3B), since it would thereby be hindered from acting as a proton donor to the second-shell methanol.[20]

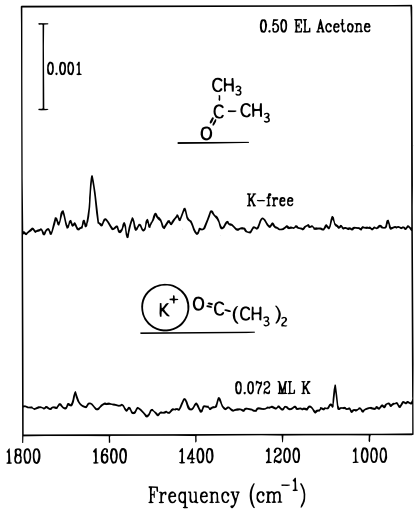

Figure 4. Mid-infrared spectra for acetone dosed onto clean and K-modified Pt(111) at 100 K. Data taken from ref 21.

While deductions along these lines are presently limited by the paucity of suitable gas-phase as well as interfacial solvation data, the value of viewing UHV double-layer modeling data as an interfacial analogy to model studies of stepwise bulk-phase solvation is nonetheless evident.

3.2. Influence of Ions upon Metal−Surface Solvation. The previous section emphasized IRAS data obtained at low solvent dosages, where ionic rather than metal−surface solvation predominates. However, UHV double-layer modeling tactics can also be utilized to provide insight into the latter issue in some cases. This is now illustrated for acetone and acetonitrile on Pt(111), specifically involving the influence of K^+ and Cl^- on the inner-layer solvent configuration.

Earlier vibrational studies using EELS as well as IRAS have identified clearly the role of the polar carbonyl and nitrile groups in binding these solvents to Pt(111).[28,29] For acetone, the carbonyl oxygen binds in a η' (vertical or tilted) configuration as depicted in the top part of Figure 4, yielding the red-shifted C═O vibration ($\nu_{C=O}$) near 1640 cm^{-1} as exemplified in the upper spectrum shown (for 0.5 EL acetone dosage) in Figure 4.[21] Acetonitrile, on the other hand, binds to Pt(111) with the cyano vibration (ν_{CN}) more strongly red-shifted (from 2270 to 1615 cm^{-1}) in the EELS spectrum, this band being absent in the IRAS data (Figure 5, upper spectrum). This confirms on the basis of the infrared selection rule that the cyano group is bound flat via π interactions.[29] Given these markedly different chemisorbed solvent orientations, it is significant that the corresponding $\Delta\Phi-\theta_s$* responses on clean Pt(111) are almost identical for acetone and acetonitrile (Figure 1D,C).[21] Coupled with the similar gas-phase dipole moments for these two molecules, the latter finding clearly emphasizes the importance of factors beyond dipole orientation in determining solvent-induced changes in the surface potential.[21]

Significantly, however, the presence of even very small K^+ coverages alters markedly the form of the infrared spectra for adsorbed acetone and acetonitrile.[21] The effect is most dramatic for the former solvent in that the $\nu_{C=O}$ band diagnostic of η' chemisorbed acetone is *removed entirely* under these conditions.

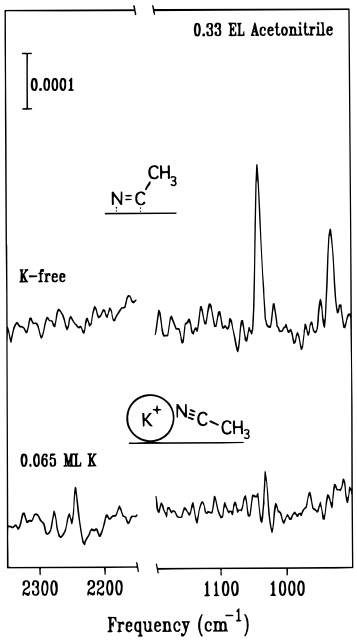

Figure 5. As for Figure 4, but for acetonitrile.

The resulting spectra as exemplified in the lower portion of Figure 4 show a complete *absence* of the chemisorbed $\nu_{C=O}$ feature, this being replaced by a weaker band near 1680 cm^{-1} which likely arises from O coordination of acetone to K^+. The removal of this chemisorbed acetone state is seen to be complete (>95%) even for θ_K values as low as 0.02. Further support for this interpretation was obtained from the observed absence of the characteristic higher-temperature TPD peak under these conditions.[21] Given that a hexagonal array of K^+ ions having a coverage of 0.02 corresponds to a nearest-neighbor separation of about 20 Å, the K^+-induced solvent reorientation must be operative over at least 2−3 solvent diameters, featuring a solvent/cation stoichiometry approaching 20![21] Such long-range perturbations can conceivably arise from ion−dipole (i.e., through-space) forces as well as by the "through-metal" class of interactions which are more often considered for UHV-based interfacial systems.[30]

The presence of K^+ also alters significantly the infrared spectra for acetonitrile, as exemplified in the lower spectrum in Figure 5. Similarly to acetone, a ν_{CN} band appeared near 2250 cm^{-1}, indicative of nitrile−cation coordination. Furthermore, the virtual loss of the C−C stretching feature at 930 cm^{-1} as well as the methyl rocking vibration at 1040 cm^{-1} in the presence of K^+ provides clear evidence that essentially the entire acetonitrile adlayer is undergoing reorientation under these conditions.[21]

The effect of adsorbed chlorine atoms, formed by gas-phase Cl_2 dosing, upon acetone chemisorption in both the absence and presence of K^+ ions was also explored;[31] such a situation involving "specifically adsorbed" (or chemisorbed) halides along with cation countercharge is commonly encountered in electrochemistry. (Note that, unlike alkali metals, chlorine adsorption is unlikely to yield fully charged ions, even when solvated, so that one can label this system as "adsorbed Cl", or $Cl^{\delta-}$.[31,32]) The presence of adsorbed chlorine was found to *stabilize* the η' acetone configuration as gleaned from an intensity enhancement of the 1640 cm^{-1} chemisorbed carbonyl band.[31] This opposite effect can be understood in terms of an attractive electrostatic interaction between the $Cl^{\delta-}$-metal image and the oriented $^{\delta+}C{=}O^{\delta-}$ dipole. However, only small (substoichiometric) K^+ coverages in the presence of coadsorbed $Cl^{\delta-}$ are required to eliminate the η' acetone state, which can be rationalized in terms of the greater ionicity of the K^+ relative to the $Cl^{\delta-}$ interfacial species.[31]

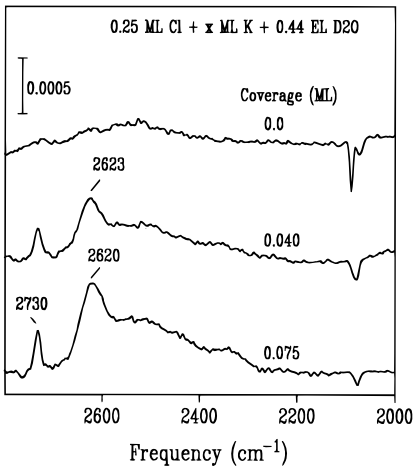

Figure 6. Effect of increasing K precoverages on infrared spectra in O−D stretch region for submonolayer D_2O dosages on Pt(111) at 100 K, also containing predosed Cl. Data taken from ref 32.

Most significantly, these results demonstrate that the inner-layer (i.e., adsorbed) solvent configuration can be drastically different in the presence of even small double-layer charges. For example, the θ_K value, 0.02, sufficient to remove entirely the η' acetone state is equivalent to a charge density of ca. 5 $\mu C\ cm^{-2}$, corresponding to an electrode potential only 50 mV or so below E_{pzc}.[33] Consequently, then, the role of ion−solvent interactions in interfacial electrochemistry can extend well beyond the shorter-range forces responsible for primary (and secondary) ionic solvation, to encompass the *entire* solvent inner layer.

3.3. Coupled Cation−Anion Solvation. While electrochemical interfaces often contain largely cation countercharges (when $E < E_{pzc}$, justifying section 3.1), as just mentioned another common circumstance involves the presence of chemisorbed halide (or other anion) adlayers together with nonspecifically adsorbed cations. It is therefore of great interest to ascertain the extent to which the solvation of the anion and cation double-layer components can be considered independently or whether marked coupling between these ostensibly separate interactions takes place. Although inherently complex, we have recently made an initial attempt to address this issue, specifically for $K^+/Cl^{\delta-}$ hydration on Pt(111). (See ref 32 for details.)

Briefly, the adsorbed Cl alone appears only to be weakly hydrated, judging by the relatively small effects seen upon the water infrared spectra, work-function, and TPD behavior except at moderate or high Cl coverages, $\theta_{Cl} > 0.25$.[32] Markedly different hydration effects are seen, however, in the presence of *both* Cl and K^+. While addition of stoichiometric amounts of Cl to adsorbed K^+ yields large Φ increases in the absence of water, suggesting intimate electrostatic $Cl^{\delta-}/K^+$ interactions, subsequent water dosing yields only minor additional Φ changes, contrasting the situation in the absence of Cl (Figure 1A). Furthermore, ν_{OD} spectral fingerprints for hydration in the presence of both $Cl^{\delta-}$ and K^+ differ substantially from corresponding spectra obtained for each double-layer solute separately. Thus, the characteristic red-shifted ν_{OD} vibrations for hydrated K^+ (Figure 2) are largely removed when $\theta_{Cl} \geq \theta_K$, and a new feature appears near 2620 cm^{-1}, most likely due to *mutual* solvation of $Cl^{\delta-}/K^+$ pairs. This finding is illustrated in Figure 6, which shows the effects upon the ν_{OD} spectra of adding K^+ cations to a partially hydrated $Cl^{\delta-}$ adlayer, which contrast the K^+ solvation effects in the absence of chlorine shown in Figure 2. Further evidence for the coupled nature of

the anion/cation hydration is also gleaned from the markedly cooperative influences of $Cl^{\delta-}/K^{+}$ adsorption observed upon the water TPD behavior.[32]

This strongly intertwined nature of the anion−cation and ion−solvent interactions is perhaps unsurprising in view of the marked coupling between ion−solvent and metal surface−solvent interactions discussed above. Taken together, however, these findings clearly attest to the inherently synergetic nature of charge-molecule−surface interactions at electrochemical interfaces. This coupling, which is not considered (or incompletely treated) in classical double-layer models, undoubtedly arises in part from the multifaceted and long-range nature of charge−dipole interfacial interactions.

4. Double-Layer Solvation of Molecular Chemisorbates

A common situation in electrochemistry entails the presence of molecular, often reactive, chemisorbates in addition to solvent and double-layer ions. While their nature can vary widely, the adsorbate having unique significance in this regard is carbon monoxide. The reasons for its importance in electrochemistry are manifold, including the common presence of adsorbed CO as a poison and/or reaction intermediate in catalytic organic electrooxidations, its well-defined and environment-sensitive vibrational properties, and the availability of a rich store of vibrational and other structural/dynamical information for CO adsorbed at metal−UHV interfaces. As already mentioned, our earlier in situ IRAS studies of adsorbed CO on monocrystalline Pt-group electrodes, which reveal substantial behavioral differences with adsorption on the corresponding clean metals in UHV,[1c,7a] provided an important initial impetus for us to undertake UHV-based electrochemical modeling studies. Moreover, the vibrational characteristics of CO, along with the related adsorbate NO, provide a valuable probe of the electrostatic properties of electrochemical in relation to UHV-based systems, especially since their intramolecular bond frequencies are sensitive to the local electric field via the so-called Stark tuning effect.[7,14]

In the remainder of this overview, we summarize some representative results of UHV double-layer modeling experiments that yield insight into how the vibrational properties of such "model molecular chemisorbates" in electrochemical systems are modified by the presence of both solvent and double-layer charges.

4.1. Charge-Free Chemisorbate Solvation. The opportunity offered by UHV electrochemical modeling to alter progressively the interfacial composition by controlling the dosage as well as multiplicity of components clearly provides an invaluable means of separating the roles of solvent and double-layer charge in altering chemisorbate properties. We will illustrate these effects primarily for the Pt(111)/CO aqueous system in view of its archetypical importance along with the availability of extensive IRAS data for the corresponding in situ electrochemical interfaces.[1c,7a,34] There are two striking differences in the vibrational characteristics for CO adsorption on clean Pt(111) (in UHV) and on Pt(111) electrodes that require explanation.[7a] First, CO binds at low coverages exclusively in atop (i.e., terminal) sites in the former case, whereas the latter environment favors 2-fold bridging or even 3-fold hollow coordination under these conditions. The spectral form, featuring C−O stretching (ν_{CO}) bands indicative of both atop and bridging configurations, only becomes similar in both environments for CO coverages approaching saturation ($\theta_{CO} \approx 0.65$). Second, even under these conditions the in situ electrochemical interface displays ν_{CO} frequencies that are markedly (40−50 cm^{-1}) lower than for the anhydrous charge-free UHV system.

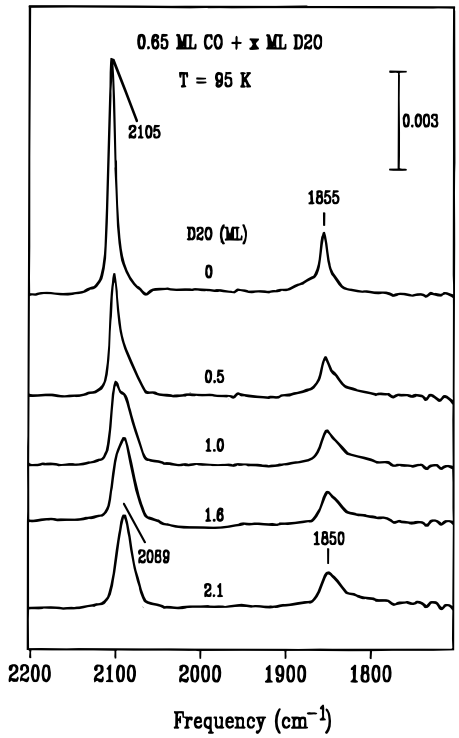

Figure 7. Effect of progressively larger D_2O dosages on infrared spectra in C−O stretching region for saturated CO adlayer on Pt(111) at 100 K. From Figure 4 of ref 16.

We consider first the effects of adding solvent in the absence of double-layer charge. Figure 7 shows the effects of progressively increasing coverages of water on the ν_{CO} spectra for a saturated CO adlayer on Pt(111) in UHV.[16] The characteristic ν_{CO} bands due to atop (2105 cm^{-1}) and bridging CO (1855 cm^{-1}) are seen to be replaced upon dosing beyond a monolayer of water by broader and red-shifted ν_{CO} features, being complete by $\theta_W \sim 2$ ML. Similar effects are seen upon the addition of several other solvents to saturated CO adlayers, although the extent of the observed red shifts, $-\Delta\nu_{CO}$, vary over the range 15−50 cm^{-1}, the $-\Delta\nu_{CO}$ values correlating with the corresponding work function decreases, $-\Delta\Phi \sim 0.5-1.8$ eV (vide infra).[16,19] Since the solvents are present as overlayers under these conditions, rather than being coadsorbed alongside CO molecules, the observed work-function decreases and corresponding Stark-shifted ν_{CO} frequencies presumably arise from charge polarization of the CO adlayer via solvent dipole or related interactions.[19,37]

More striking solvent-induced alterations in the ν_{CO} spectra are uniformly observed at low or moderate CO coverages ($\theta_{CO} < 0.4$), as exemplified by the solvent-dosing sequence for methanol onto 0.25 monolayer (ML) of CO shown in Figure 8.[35] The addition of ca. 0.6 EL of methanol, corresponding to a methanol/CO stoichiometric ratio of around unity, is sufficient to remove entirely the atop ν_{CO} band and replace it with a broader and weaker ν_{CO} feature at 1805−1810 cm^{-1} associated with bridging CO. Again, comparable effects are seen with several other solvents, although in some cases, such as acetonitrile and water, a full solvent monolayer is required to complete the ν_{CO} spectral transformation.[35,36]

Significantly, this solvent-induced shift in CO binding site accounts for the first major difference between the conventional UHV and electrochemical interfaces noted above. The effect has been suggested to arise from juxtaposed adsorbed CO and solvent molecules acting to stabilize the otherwise less favored bridging CO geometry via dipolar interactions.[35,36] In addition, the marked attenuation of the ν_{CO} band intensity in the bridging

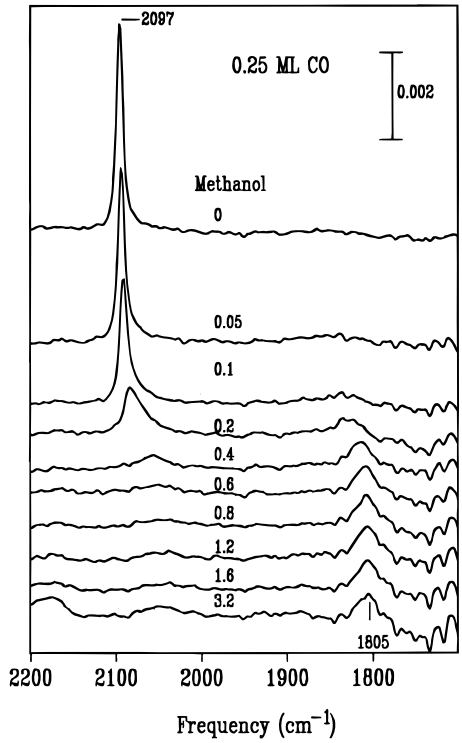

Figure 8. Effect of progressively larger methanol dosages on infrared spectra for subsaturated CO adlayer on Pt(111) at 100 K. From Figure 1 of ref 35.

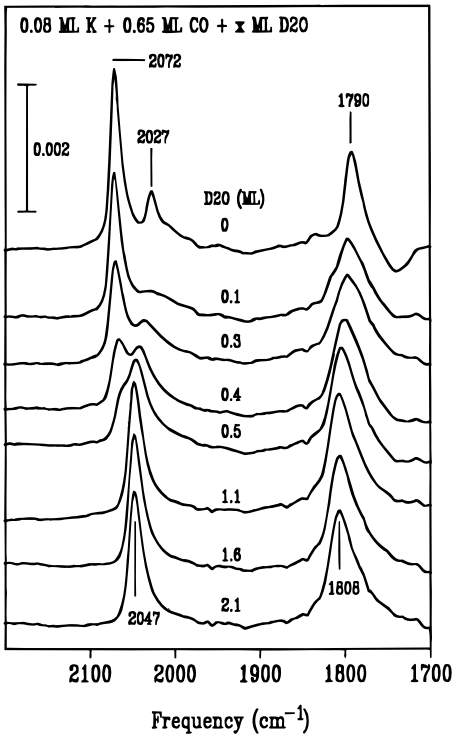

Figure 9. Effect of progressively large D_2O coverages on infrared spectra for saturated CO adlayer on Pt(111) at 100 K with predosed K. From Figure 6 of ref 16.

configuration can be accounted for in terms of solvent dielectric screening.[35] It is interesting to note, however, that the CO−water interactions on Pt(111) have been characterized as "hydrophobic" by Wagner et al. on the basis of the observed lowering of the water desorption temperature upon the addition of adsorbed CO.[6a,43] While the TPD effect may be due in part to a CO-induced diminution of water hydrogen bonding, it suggests that the water-induced CO site shifting may be due to a preferential solvent blocking of the atop sites rather than a stabilization of the CO bridging geometry. This notion can indeed account for the required presence of a full water monolayer to switch the CO binding site.

The addition of water to a saturated NO adlayer on Pt(111) similarly yields red shifts in the frequency of the single ν_{NO} band, presumably due to atop NO, along with corresponding work-function decreases.[13] A difference with the CO case, however, is that no solvent-induced change in adsorbate binding site appears to occur at lower NO coverages, θ_{NO}, the observed ν_{NO} frequency red shifts being roughly compatible with the Stark shift anticipated from the observed $-\Delta\Phi$ changes.[13] A likely reason for this behavioral difference, however, is that multifold NO binding appears to be preferred at lower θ_{NO} values even in the *absence* of solvent, in contrast to the preference for atop binding with CO under these conditions.

4.2. Effects of Double-Layer Charge. Work-function measurements undertaken for the Pt(111)/CO system after solvent addition yield Φ values, chiefly in the range ca. 4.5−5.5 eV, that tend to be higher than those typically encountered in electrochemical environments.[19] For example, water addition onto a saturated CO adlayer yields $\Phi \approx 5.6$ eV,[16] which from eq 1 corresponds to $E^M \approx 1.0$ V vs NHE if E_k is taken as 4.6 V (vide supra). This E^M value is indeed well above that accessible for saturated Pt(111)/CO adlayers in ambient-temperature acidic aqueous solution, CO electrooxidation commencing by about 0.55 V vs NHE.[34] (The lack of CO oxidation in the low-temperature aqueous UHV environment is undoubtedly due to kinetic restrictions.) Given that the Pt(111)/CO,-water−UHV interface in the absence of charges necessarily refers to E_{pzc}, one deduces that the corresponding electrochemical interface carries negative electrode charges under most conditions. Consequently, then, it is appropriate to examine double-layer charging effects in the UHV model system by adding potassium as well as solvent as considered above, K^+ ions being formed along with the negative metal electronic charge.

Figure 9 shows the effects of adding increasing water dosages onto a saturated CO adlayer on Pt(111) also containing a moderate K coverage, 0.08 ML.[15,16] The top spectrum, obtained prior to water addition, is usefully compared with the corresponding K^+-free spectrum in Figure 7 (top). The presence of K^+ in the absence of water is seen to generate a new ν_{CO} band at 2027 cm^{-1} as well as red-shifting markedly (by 30 and 65 cm^{-1}, respectively) the atop and bridging ν_{CO} features. These effects have been ascribed to the presence of specific short-range, as well as longer-range, electrostatic interactions.[38] Subsequent water additions, as seen in Figure 9, act to modify substantially such complex K^+−CO forces. Thus, dosing even small amounts of water, corresponding to water/K^+ stoichiometries of 1−2, essentially *removes* the "short-range" ν_{CO} feature at 2027 cm^{-1}. Adding larger amounts of water, ca. one monolayer, so that solvation of the CO adlayer as well as the K^+ ions is completed, is seen to modify substantially the frequencies of the "major" atop and bridging features (Figure 9). Indeed, the addition of increasing K^+ coverages to a CO adlayer fully solvated (say, $\theta_s > 2$) with water or other solvents yields progressively larger monotonic downshifts (i.e., Stark shifts) of the atop and bridging ν_{CO} features, just as are observed for the in situ electrochemical interfaces (vide infra).[15]

A more striking illustration of the mediating influence of double-layer solvation on chemisorbate−cation interactions is seen in Figure 10A,B, comparing the effects of K^+ addition upon the ν_{CO} spectra at a lower CO coverage, 0.25 ML, in the absence (A) and presence (B) of water. In the former case, K^+ addition is seen to yield large and complex effects upon the

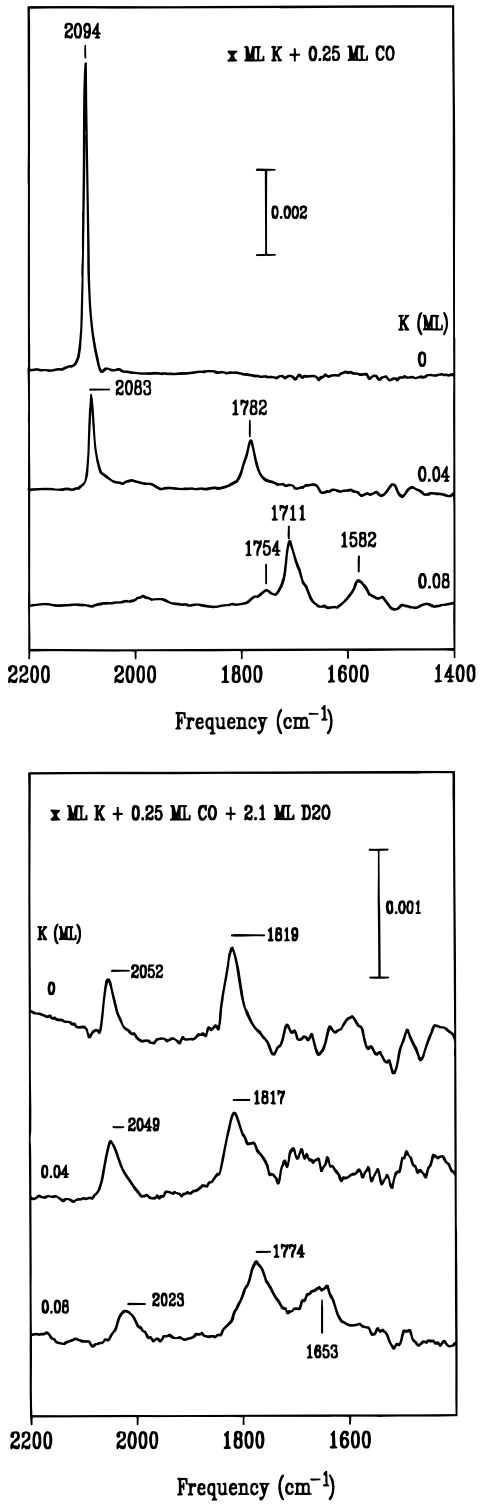

Figure 10. Effect of increasing K coverages on infrared spectra for subsaturated CO adlayer on Pt(111) at 100 K in the (A) absence and (B) presence of water (2 monolayers). From Figure 9 of ref 16.

ν_{CO} spectra, the "normal" atop ν_{CO} band being replaced by a series of strongly red-shifted features around 1580−1750 cm^{-1} (Figure 10A), apparently indicative of dominant "short-range" K^+− CO interactions.[38] A markedly simpler response, however, is observed in the hydrated interfacial environment, K^+ addition merely yielding progressive Stark-like downshifts of the atop and bridging ν_{CO} bands that are formed upon water addition in the absence of cationic charge (Figure 10B).

Consequently, then, solvation of the *charge-free* CO adlayer is responsible for the marked differences in binding-site occupancy between the electrochemical and conventional UHV

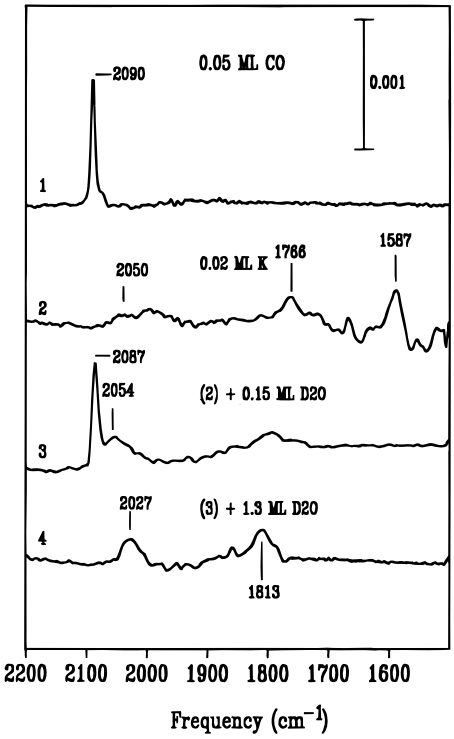

Figure 11. Effect on infrared spectra on Pt(111) at 100 K for low CO coverage (0.05 monolayer) of sequentially adding potassium and then water coverages indicated. From Figure 11 of ref 16.

environments, the addition of double-layer charge in the presence of solvent being simply to generate the ν_{CO} frequency downshifts that also characterize the former interface in comparison with the latter.[15] This remarkable simplification of the effects of ionic charge upon chemisorbate properties engendered by the presence of solvent can be attributed primarily to the elimination of short-range K^+−CO forces by preferential cation solvation. The modification of apparent longer-range K^+−CO interactions by solvation, as suggested in Figure 9, may be due to relocation of the cations above the CO layer brought about by complete hydration. Another important factor, however, is probably the dielectric screening induced by the presence of complete ($\theta_s \geq 2$ ML) double-layer solvation, as also suggested by the markedly smaller Φ decreases triggered by K^+ addition in the presence compared with the absence of solvent.[15,16,33] (cf. Figure 1A−D). These findings can indeed account for the otherwise-surprising success of "average-potential" models in classical electrochemistry, especially concerning diffuse-layer effects in electrode kinetics and double-layer structure,[39] in that the (strictly discrete) ionic charges can nevertheless be described approximately as being "smeared out" parallel to the metal−solution interface.

Further insight into the nature of preferential solvation effects can be gleaned from UHV double-layer modeling measurements, involving sequential chemisorbate, cation, and solvent additions at very low coverages, so that there is a ready availability of metal surface sites. Figure 11 is an example of such an experiment.[16] The top spectrum (1), for a very low CO coverage (0.05 ML) on clean Pt(111), is seen to be modified drastically by the addition of even a substoichiometric K coverage, 0.02 (spectrum 2, cf. Figure 10A). Interestingly, the subsequent addition of sufficient water to completely solvate the cations, 0.15 ML, but *not* the remaining surface not only essentially removes the low-frequency ν_{CO} features diagnostic of short-range K^+−CO interactions but also largely *regenerates* the unshifted atop ν_{CO} based seen originally on the clean surface (spectrum 3).

This last finding suggests that the hydrated K^+ and adsorbed CO are forming largely *spatially separated domains* on the metal surface, so that the unsolvated CO becomes largely unaffected by the cationic charge. The implied weak CO−water interaction is consistent with the observed destabilization of adsorbed water in the presence of CO as deduced by TPD measurements (vide supra).[6a,43] Nevertheless, addition of a full water monolayer, so that the entire surface (including the CO) becomes hydrated, triggers a further drastic change in the chemisorbate configuration, the familiar spectral fingerprints for the "normal electrochemical" interface being generated, featuring extensive site transfer along with substantial cation-induced ν_{CO} frequency downshifts (spectrum 4). Taking the findings of Figures 7−11 together, it is apparent that the "Stark-tuning effect" familiar in electrochemistry, associated with variations in the electrode potential and hence the double-layer charge, results from the occurrence of solvation of *both* the ions and the chemisorbate.

5. Quantitative Comparisons with in Situ Electrochemical Interfaces

As noted above, an important part of the UHV double-layer modeling approach involves quantitative comparisons with the behavior of actual (i.e., in situ) electrochemical interfaces. Such comparisons not only provide a validation (or otherwise!) of the UHV-modeling approach but also can yield firm ties between the electrochemical and UHV-based branches of surface science. So far, such comparisons have largely been of two types, involving either (a) charge−potential behavior and/or (b) potential-dependent vibrational spectroscopy of chemisorbates.[4−6]

The former type of intercomparisons are obviously most useful for surfaces, such as gold and silver, for which reliable in situ measurements of the double-layer capacitance can be made, therefore enabling potentials of zero charge and hence electrode charge−potential data to be set alongside the corresponding UHV-based behavior.[6] For example, Sass, Parsons, and co-workers undertook a detailed comparison between the adsorption thermodynamics of bromide at the Ag(110)−aqueous electrochemical interface and related UHV-based work function−interfacial composition measurements involving Br adsorption on Ag(110) in the presence of varying water dosages.[40] As discussed in detail by Wagner,[6a] the best concordance between the electrochemical and UHV-based data is found for water dosages around a monolayer, suggesting that the inner-layer solvent (and primary solute solvation) provides the critical element of the surface potential for electrochemical systems. Other examinations along these general lines include an investigation into the role of hydrogen/water coadsorption on Pt(111) in the voltammetric properties of the Pt(111)−acidic aqueous interface.[6a] While the low temperatures obliged for the UHV model experiments can alter such double-layer and voltammetric properties, especially kinetically limited phenomena, it should be noted that Stimming and co-workers have found that such measurements at metal−aqueous interfaces are essentially *unaffected* by freezing the solution.[44]

While the difficulties in extracting reliable in situ charge−electrode potential data on transition-metal surfaces limit the quantitative scope of such comparison with UHV model interfaces, it is nonetheless instructive to scrutinize $\Delta\Phi-$composition data for the latter systems as a means of assessing the electrostatic roles of solvation in electrochemical interfaces. Thus, examining $\Delta\Phi-\theta_K$ (i.e., surface potential−charge) relationships for the Pt(111)−solvent interfaces depicted in Figure 1 (derived by taking vertical "slices" through the $\Delta\Phi-\theta_s$* profiles for different θ_K values) shows that both primary ionic and metal surface solvation forge the capacitive characteristics of in situ electrochemical systems (vide supra).[33]

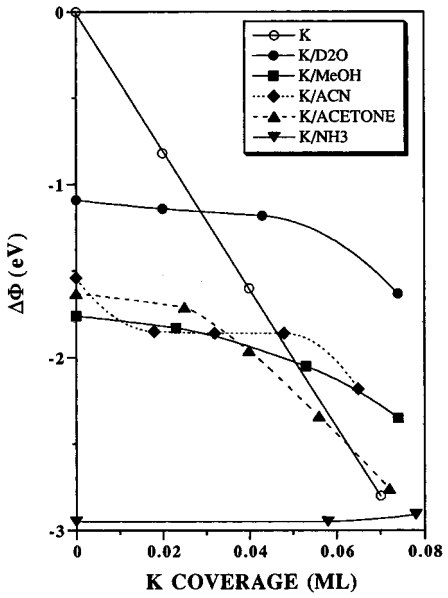

Figure 12. Plots of work-function changes induced on Pt(111) at 100 K as a function of K coverage in the presence of various multilayer solvents, as indicated. Data taken from ref 33.

As an illustrative example, Figure 12 shows $\Delta\Phi-\theta_K$ data for five UHV-based Pt(111)−solvent interfaces, as indicated, in comparison with the corresponding response in the complete absence of solvent (open circles). [Note that the $\Delta\Phi$ measurements are again referenced to the Φ value, 5.9 eV, for clean Pt(111).] Generally speaking, with the exception of ammonia, the $\Delta\Phi-\theta_K$ profiles are not greatly dependent on the nature of the solvent, apart from variations in E_{pzc} (appearing as the y intercept in Figure 12). They are, of course, very different to the solvent-free case. (Recall that the inverse slopes of these plots are proportional to the double-layer capacitance, C_{dl}.) This indicates that the dielectric screening properties are not especially sensitive to the solvent molecular structure, C_{dl} values around 15−30 μF cm^{-2} being deduced from the $\theta_K-\Delta\Phi$ slopes.[33] Such a finding is a familiar one to electrochemists.[41] The near-zero $\Delta\Phi-\theta_K$ slope (i.e., very high apparent C_{dl} value) obtained with ammonia is believed to be due to "redox pinning", associated with the formation of K^+-solvated electron pairs at the very low surface potentials achieved with this solvent.[33,42]

The second type of comparison between UHV model and in situ electrochemical interfaces noted above, (b), involving potential-dependent vibrational data, is most readily undertaken for transition-metal surfaces in view of their chemisorbing ability. Following from the discussion in the last section, we illustrate briefly this notion with reference to saturated CO adlayers at solvated Pt(111)/K^+ interfaces. Figure 13 contains plots of the frequency for the atop ν_{CO} band, ν_{CO}^{atop}, versus the work function for five solvated UHV interfaces, as indicated, along with corresponding $\nu_{CO}^{atop}-\Phi$ data for the in situ Pt(111)−acidic aqueous interface.[15] [The E^M values for the in situ interface were converted into Φ values by using eq 1, assuming that $E_k = 4.6$ V vs NHE.] The UHV solvent dosages in each case correspond to the point (θ_s* ≈ 1−2 ML) above which no further ν_{CO} spectral changes occurred. The highest ν_{CO} frequency (and Φ value) in each solvent refers to the uncharged Pt(111)−UHV interface, with decreasing values corresponding to progressively higher θ_K values, up to ca. 0.08 ML.

The significant feature of Figure 13 is that essentially linear $\nu_{CO}^{atop}-\Phi$ "Stark-tuning" plots are obtained in each case, which, moreover, are largely *independent* of the solvating medium,

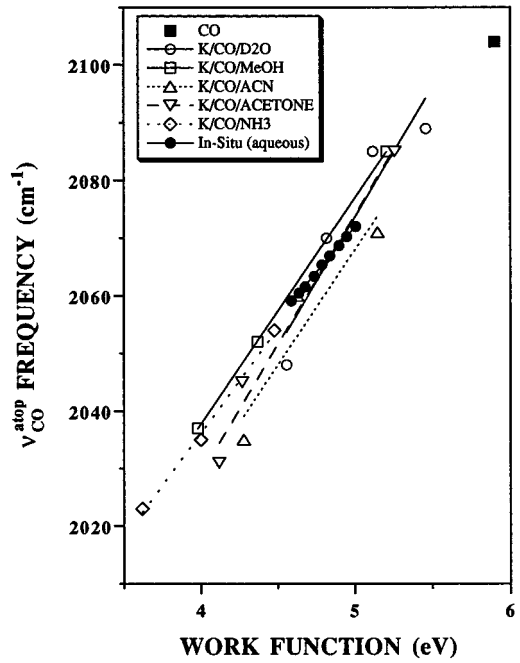

Figure 13. Infrared band frequency for atop CO in a saturated adlayer on Pt(111) at 100 K modified by the various solvents indicated and with varying K coverages plotted against the surface work function. See text for details. Taken from ref 15.

yielding a slope of about 35 cm^{-1} eV^{-1}. The in situ data are also concordant when choosing the E_k value, 4.6 ± 0.2 V. Indeed, it was noted earlier that the in situ frequency-electrode potential IRAS data are also essentially independent of the solvent once the appropriate liquid-junction potentials (vs the reference electrode) are taken into account.[8a] Roughly comparable findings are obtained for the bridging ν_{CO} band, although this feature displays somewhat more complex behavior.[8a,15,16]

Consequently, then, one deduces that the molecular nature of the solvent is unimportant in influencing the CO adlayer vibrational properties once its effect on altering the work function (and hence the surface potential) is assessed. This result appears reasonable provided a large fraction of the surface-potential drop falls across the CO adlayer, since the Stark-tuning effect should be controlled by the surface charge and attendant variations in electrostatic field sensed by the chemisorbate.[14] It is, nonetheless, worth recalling that the ν_{CO} frequency and the corresponding Φ downshifts, induced by solvent addition in the absence of charge, are distinctly solvent *dependent* (ΔΦ values from 0.5 to 1.7 eV). Therefore, the specific solvent nature does affect the observed Stark tuning, even though the additional *charge-induced* component is relatively solvent *insensitive*.[15]

6. General Conclusions and Future Prospects

Although the UHV-based electrochemical modeling approach has been pursued avidly so far by relatively few groups, most notably those of Stuve and Wagner as well as Sass,[4−6] it is evident that such tactics have much to offer electrochemists and other surface scientists in their quest to unravel the intricacies of the complex multicomponent interfaces that abound in condensed-phase surface chemistry. While the usual obligation to employ lower temperatures in the UHV experiments might be construed as a serious weakness, a crucial value of the approach is to identify the fundamental manner in which the various components contribute to the physical (and chemical) properties of the interface as a whole, rather than provide a perfect facsimile of the in situ system.[6] Perhaps equally importantly, harnessing the powerful swath of UHV-based techniques to explore related metal−liquid, as well as metal−vacuum, interfaces in this fashion will not only furnish fresh perspectives into electrochemical phenomena but also should encourage a greater commonality of purpose in these formerly segregated branches of surface science.

The recent explosive growth in powerful microscopic-level techniques applicable to in situ solid−liquid interfaces is providing an increasingly rich body of structural and dynamical information, in some cases even on a par with that achieved for metal−UHV systems. Rather than discouraging model UHV studies, however, these in situ developments are *encouraging* such approaches as a unique means of understanding the factors that control the behavior of solid−liquid interfaces in relation to their (often simpler) solid−UHV counterparts. This is especially true when the same microscopic-level properties can be examined in the in situ and UHV-based environments, such as chemisorbate vibrational characteristics or real-space molecular structure.[45] While the range of adsorbate and interfacial systems amenable to such analyses is restricted, in particular, by remaining limitations of the in situ methods (for example, bulk-phase solvent interferences in IRAS), the depth of physical insight to be gained in this fashion provides a strong impetus encouraging its further development.

What, then, are some issues in electrochemical surface science that could benefit from a continuing evolution of UHV-based modeling studies? One important unresolved question concerns the manner and extent to which the surface-potential profile is influenced by solvent adsorption. So far, most measurements indicate that substantial (>0.5 eV) work-function decreases are induced by adsorption of water as well as other solvents on clean metals in UHV [6a,10] (cf. Figure 1). While these low-temperature (<150 K) findings imply that the inner-layer solvent substantially influences E_{pzc}, this deduction has been questioned, primarily on the basis of comparisons between corresponding Φ and E_{pzc} values along with the belief held by some that the −ΔΦ values should be markedly smaller at ambient-temperature electrochemical interfaces.[10] (See, however, ref 19 for an alternative view.) Given this uncertainty (due partly to doubts concerning the E_k value), it would clearly be worthwhile to undertake ΔΦ measurements at higher, even approaching ambient, temperatures by employing greatly increased solvent pressures.

In addition, however, it would be extremely desirable to undertake further UHV-based ΔΦ measurements for solvent addition in the presence of anion as well as cations that are known to be "nonspecifically adsorbed" (i.e., retain their solvation shells) at electrochemical interfaces. One motivation is that the double layer contains both cations and anions (albeit at low coverages) even at the potential of zero charge (E_{pzc}), which may therefore affect the solvent-induced ΔΦ values. Double-layer modeling studies involving suitable anions, such as perchlorate or possibly fluoride, are rare so far, although feasible.[6] More generally, it would be interesting to examine further the vibrational as well as ΔΦ properties of nonaqueous solvents as well as water in the presence of varying ratios of such anions and cations, mimicking the double-layer composition at potentials above as well as below E_{pzc}. The recent upsurge in diverse studies of progressive ionic and molecular solvation in the gas phase[46] also provides a strong incentive to develop further analogous measurements of interfacial solvation. Of particular interest is the nature of anion and neutral adsorbate as well as cation solvation and how the presence of each species in the double layer mutually affects their solvated structure.

While the use of low-temperature conditions obliged in most UHV double-layer modeling studies is in a sense a restriction,

this could also be turned to an advantage in expanding considerably the temperature range over which electrochemical phenomena may be explored. For example, the greatly diminished mobility of adsorbates under such conditions provides intriguing opportunities for the examination of ordered adlayer structure, especially by using STM. A distinctly different, yet also largely untapped, research direction in this vein involves kinetic studies of interfacial charge-transfer phenomena. Such processes could readily be initiated by either photoemission or alterations in surface potential induced by gas-phase dosing and followed by spectroscopic means. The opportunity to vary the surface temperature over much wider ranges than attainable for conventional electrified interfaces, along with the ability to alter systematically the interfacial structure and composition (including the extent of solvation), could yield truly novel insight into charge-transfer phenomena.

Overall, then, there are manifold reasons to anticipate that UHV-based measurements utilizing such double-layer modeling tactics, along with ex situ electrode-transfer approaches, should contribute increasingly to our fundamental understanding of electrochemical phenomena in the near future. Especially when pursued in parallel with in situ microscopic-level techniques, such studies stand to provide a much more unified as well as richer understanding of surface chemical behavior.

Acknowledgment. Naushad Kizhakevariam contributed greatly to the initial phase of these studies through his experimental craftsmanship as well as fundamental data interpretation. This research is supported by the National Science Foundation.

References and Notes

(1) For overviews see: (a) Weaver, M. J. *J. Phys. Chem.* **1996**, *100*, 13079. (b) Weaver, M. J.; Gao, X. *Annu. Rev. Phys. Chem*, **1993**, *44*, 459. (c) Chang, S.-C.; Weaver, M. J. *J. Phys. Chem*. **1991**, *95*, 5391.

(2) For broad-based reviews, see: (a) *Structure of Electrified Interfaces*; Lipkowski, J., Ross, P. N., Eds.; VCH Publishers: New York, 1993. (b) *Comprehensive Chemical Kinetics*; Compton, R. G., Hamnett, A., Eds.; Elsevier: Amsterdam, 1989; Vol. 29. (c) *Electrochemical Interfaces: Modern Techniques for In-Situ Interface Characterization*; Abruna, H. D., Ed.; VCH Publishers: New York, 1991.

(3) Hubbard, A. T. *Chem. Rev*. **1988**, *88*, 633.

(4) Stuve, E. M.; Krasnopoler, A.; Sauer, D. E. *Surf. Sci*. **1995**, *335*, 177.

(5) (a) Sass, J. K.; Bange, K. *ACS Symp. Ser*. **1988,** *378*, 54. (b) Sass, J. K.; Bange, K.; Döhl, R.; Piltz, E.; Unwin, R. *Ber. Bunsen-Ges. Phys. Chem*. **1984**, *88*, 354.

(6) For recent erudite reviews see: (a) Wagner., F. T. In ref 2a, Chapter 9. (b) Stuve, E. M.; Kizhakevariam, N. *J. Vac. Sci. Technol. A* **1993**, *11*, 2217.

(7) Chang, S.-C.; Weaver, M. J. *Surf. Sci.* **1990**, *238*, 142. (b) Weaver, M. J. *Appl. Surf. Sci*. **1993**, *67*, 147.

(8) Chang, S.-C.; Jiang, X.; Roth, J. D.; Weaver, M. J. *J. Phys. Chem*. **1991**, *95*, 5378. (b) Jiang, X.; Weaver, M. J. *Surf. Sci*. **1992**, *275*, 237.

(9) (a) Trasatti, S. *J. Electroanal. Chem*. **1983**, *150*, 1; **1982**, 139, 1. (b) Trasatti, S. *Electrochim. Acta* **1983**, *28*, 1083. (c) Trasatti, S. *Electrochim. Acta* **1990**, *35*, 269.

(10) Trasatti, S. *Electrochim. Acta* **1991**, *36*, 1659.

(11) For example, see: Hansen, W. N.; Hansen, G. J. *ACS Symp. Ser*. **1988**, *378*, 166.

(12) Samec, Z.; Johnson, B. W.; Doblhofer, K. *Surf. Sci*. **1992**, *264*, 440.

(13) Villegas, I.; Gomez, R.; Weaver, M. J. *J. Phys. Chem*. **1995**, *99*, 14832.

(14) For an overview, see: Lambert, D. K. *Electrochim. Acta* **1996**, *41*, 623.

(15) Villegas, I.; Weaver, M. J. *J. Phys. Chem. B* **1997**, *101*, 5842.

(16) Kizhakevariam, N.; Villegas, I.; Weaver, M. J. *J. Phys. Chem*. **1995**, *99*, 7677.

(17) Pirug, G.; Bonzel, H. P. In ref 2a, Chapter 5.

(18) (a) Pirug, G.; Bonzel, H. P. *Surf. Sci*. **1988**, *194*, 159. (b) Bonzel, H. P.; Pirug, G.; Ritke, C. *Langmuir* **1991**, *7*, 3066.

(19) Kizhakevariam, N.; Villegas, I.; Weaver, M. J. *Surf. Sci*. **1995**, *336*, 37.

(20) Villegas, I.; Weaver, M. J. *J. Chem. Phys.* **1995**, *103*, 2295.

(21) Villegas, I.; Weaver, M. J. *J. Am. Chem. Soc*. **1996**, *118*, 458.

(22) Note that the solvent dosages are given in "equivalent layers" (EL), where a unit EL value refers to a close-packed solvent monolayer as gleaned from TPD measurements. These "coverages" (θ_s*) differ from those quoted here for potassium (θ_K) which are referenced instead to the surface metal atomic density, 1.5×10^{15} atoms cm^{-2} (see, for example, refs 20 and 21).

(23) Sass, J. K.; Lackey, D.; Schott, J. *Electrochim. Acta* **1991**, *36*, 1883.

(24) Willey, K. F.; Yeh, C. S.; Robbins, D. L.; Pilgrim, J. S.; Duncan, M. A. *J. Chem. Phys.* **1992**, *97*, 8886.

(25) Baumann, P.; Pirug, G.; Reuter, D.; Bonzel, H. P. *Surf. Sci*. **1995**, *335*, 186.

(26) (a) Selegue, T. J.; Moe, N.; Draves, J. A.; Lisy, J. M. *J. Chem. Phys*. **1992**, *96*, 7268. (b) Draves, J. J.; Luthey-Schulten, Z.; Liu, W.-L.; Lisy, J. M. *J. Chem. Phys*. **1990**, *93*, 4589.

(27) LaCosse, J. P.; Lisy, J. M. *J. Phys. Chem*. **1990**, *94*, 4398.

(28) (a) Vannice, M. A.; Erley, W.; Ibach, H. *Surf. Sci*. **1991**, *254*, 1. (b) Anton, A. B.; Avery, N. R.; Toby, B. H.; Weinberg, W. H. *J. Am. Chem. Soc*. **1986**, *108*, 684.

(29) (a) Ou, E. C.; Young, P. A.; Norton, P. R. *Surf. Sci*. **1992**, *277*, 123. (b) Sexton, B. A.; Avery, N. R. *Surf. Sci*. **1983**, *129*, 21.

(30) See for example: Norskov, J. K. In *The Chemical Physics of Solid Surfaces*; King, D. A., Woodruff, D. P., Eds.; Elsevier: Amsterdam, 1993; Vol. 6, Chapter 6.

(31) Villegas, I.; Weaver, M. J. *J. Electroanal Chem*. **1997**, *426*, 55.

(32) Villegas, I.; Weaver, M. J. *J. Phys. Chem*. **1996,** *100*, 19502.

(33) Weaver, M. J.; Villegas, I. *Langmuir*, in press.

(34) Chang, S.-C.; Weaver, M. J. *J. Chem. Phys.* **1990**, *92*, 4582.

(35) Kizhakevariam, N.; Villegas, I.; Weaver, M. J. *Langmuir* **1995**, *11*, 2777.

(36) Kizhakevariam, N.; Jiang, X.; Weaver, M. J. *J. Chem. Phys*. **1994**, *150*, 6750.

(37) Xu, Z.; Yates, J. T.; Wang, L. C.; Kreuzer, H. J. *J. Chem. Phys*. **1986**, *85*, 4153.

(38) Tüshaus, M.; Gardner, P.; Bradshaw, A. M. *Surf. Sci*. **1993**, *286*, 212.

(39) For example, see: Delahay, P. *Double Layer and Electrode Kinetics*; Wiley: New York, 1965.

(40) Bange, K.; Straehler, B.; Sass, J. K.; Parsons, R. *J. Electroanal. Chem*. **1987**, *229*, 87.

(41) For example, see: (a) Trasatti, S. In *Modern Aspects of Electrochemistry*; Conway, B. E., Bockris, J. O'M., Eds.; Plenum: New York, 1979; Vol. 13, Chapter 2. (b) Reeves, R. In *Comprehensive Treatise of Electrochemistry*; Bockris, J. O'M., Conway, B. E., Yeager, E., Eds.; Plenum: New York, 1980; Vol. 1, Chapter 3.

(42) Villegas, I.; Weaver, M. J. *Surf. Sci*. **1996**, *367*, 162.

(43) Wagner, F. T.; Moylan, T. E.; Schmeig, S. J. *Surf. Sci*. **1988**, *195*, 403.

(44) Borkowska, Z.; Stimming, U. In ref 2a, Chapter 8.

(45) Villegas, I.; Weaver, M. J. *J. Chem. Phys.* **1994**, *101*, 1648.

(46) For recent overviews, see: (a) Zwier, T. S. *Annu. Rev. Phys. Chem*. **1996**, *47*, 205. (b) Castleman, Jr., A. W.; Bowen, Jr., K. H. *J. Phys. Chem*. **1996**, *100*, 12911.